2nd URSI AT-RASC, Gran Canaria, 28 May – 1 June 2018

From Doppler to FMCW Radars for Non-Contact Vital-Sign Monitoring

José-María Muñoz-Ferreras(1), Jing Wang(2), Zhengyu Peng(2), Roberto Gómez-García(1), and Changzhi Li(2)
(1) Dept. of Signal Theory & Communications, University of Alcalá, 28871 Alcalá de Henares, Spain
(2) Dept. of Electrical & Computer Engineering, Texas Tech University, Lubbock, TX 79409, USA

Abstract

Contactless monitoring of vital signs (e.g., respiration and heartbeats) is gaining a high interest in biomedical and healthcare applications. To that purpose, radar systems are very desired due to their unique characteristics in terms of improved sensitivity to detect small vibrations. This work reviews the traditional Doppler architecture for biomedical short-range radars and presents the recently-proposed coherent frequency-modulated continuous-wave (FMCW) scheme for improved vital-sign-monitoring tasks. The advantages of the FMCW solution in comparison with Doppler radars are emphasized. Experimental results from custom-designed and manufactured prototypes are also shown.

1 Introduction

Non-contact detection and monitoring of vital signs have a large importance in several scenarios, e.g., the detection of life after avalanches or earthquakes, seniorcare at home, the monitoring of sleep, the care of patients that cannot use contact devices, and so forth [1]. In addition to optical techniques such as photoplethysmography [2], radar systems are very-desired candidates for contactless vital-sign-monitoring applications due to their unique features to detect small vibrations [3].

Doppler radars transmit a single continuous-wave (CW) tone. The received echo is mixed with a replica of the transmitted signal, leading to the in-phase and quadrature (I/Q) components of the baseband signal, whose phase is related with the vital signs. Since the first application of Doppler radars to monitor vital signs of animals [4], many efforts have been devoted to improve their architectures. For example, DC-coupled schemes have been investigated to avoid distortion of the low-frequency components of the vital signs and low-intermediate-frequency (low-IF) solutions have been approached to circumvent issues regarding undesired flicker noise and saturating DC offsets [5].

However, Doppler radars still have critical limitations. Since they do not possess range resolution, moving targets at other ranges mean an important interference for them. Also, they cannot simultaneously handle the vital signs of multiple illuminated patients. Recently, coherent deramping-based frequency-modulated continuous-wave (FMCW) radar systems have been proposed to alleviate the aforementioned drawbacks at a very reduced cost [6].

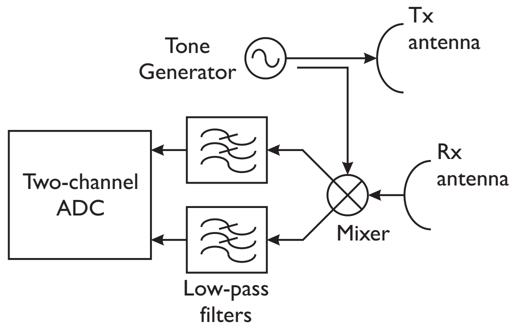

Figure 1. High-level schematic for a biomedical Doppler radar system (Tx: transmission, Rx: reception, ADC: analog-to-digital converter).

This manuscript reviews the theoretical fundamentals of Doppler and FMCW radar systems for vital-sign monitoring. In addition, experimental results from custom-designed and manufactured radar prototypes are also shown and discussed.

2 Theoretical Foundations

This section provides the mathematical foundations of biomedical short-range Doppler and FMCW radars. From this theory, the features of each architecture together with their associated signal-processing tasks required to obtain the desired vital signs are inferred.

2.1 Biomedical Doppler Radars

A high-level schematic for a biomedical Doppler radar is detailed in Fig. 1. To minimize the undesired RF coupling between the transmitter and the receiver, the scheme uses two antennas. Note also that a replica of the transmitted CW sinusoidal signal is mixed in quadrature with the received echoes to obtain the I/Q components. These baseband signals I and Q are low-pass filtered and subsequently acquired by a low-end two-channel analog-to-digital converter (ADC).

The complex-valued analytic expression for the transmitted signal $s_{Tx}^{A}(t)$, where the super-index A refers to this Doppler operation mode, can be written as

$$s_{Tx}^{A}(t) = \exp(j2\pi f_0 t) \tag{1}$$

where f_0 is the operation frequency and t is the time. For simplicity, a unity amplitude has been considered.

Assume that the Doppler radar illuminates a moving point-scatterer whose range is given by $R(t)$. The received signal can be mathematically expressed as

$$s_{Rx}^{A}(t) = \sigma \cdot s_{Tx}^{A}\left(t - \frac{2R(t)}{c}\right) \tag{2}$$

where σ is its amplitude and c is the speed of light.

After the demodulation process and low-pass filtering in Fig. 1, the baseband signal $s_b^A(t)$ for the illuminated point scatterer can be expressed as

$$s_b^A(t) = s_{Tx}^{A}(t) \cdot \left(s_{Rx}^{A}(t)\right)^* = \sigma \exp\left(j\frac{4\pi f_0}{c}R(t)\right) \tag{3}$$

where * indicates complex conjugate.

From (3), it comes to light that the range history of the target $R(t)$ can be estimated from the phase measurements $\phi(t)$ of the baseband signal, as follows:

$$\hat{R}(t) = \frac{c}{4\pi f_0}\phi(t). \tag{4}$$

The indicated estimation of the range history of the vital signs requires unwrapping of the phase. Also, since the phase is ambiguous in the range 2π, it can be deduced from (4) that Doppler radars have a very small non-ambiguous range of $c/(2f_0)$. In addition, note that Doppler radars do not possess range resolution and that they are very sensitive to undesired moving clutter.

2.2 Biomedical FMCW Radars

A high-level schematic for a biomedical FMCW radar is depicted in Fig. 2. Given the fact that the waveform is of continuous type, two antennas are again employed to minimize Tx/Rx coupling. Also, a replica of the transmitted signal is mixed with the returned echoes to give rise to the so-called beat signal. This signal is low-pass filtered and digitalized by a low-end cost-efficient ADC.

Fig. 3 depicts the conventional sawtooth waveform for an FMCW radar [6]. The instantaneous bandwidth is given by B, the period is T, and the center frequency is designated by f_c. Referring to Fig. 2, the generation of the frequency ramps can be accomplished through excitation of the free-running voltage-controlled oscillator (VCO) with operational-amplifier-based periodic linear voltages. In the case that the VCO has a non-linear frequency-voltage curve, the controlling voltage could be adequately modified to improve the linearity of the RF ramps.

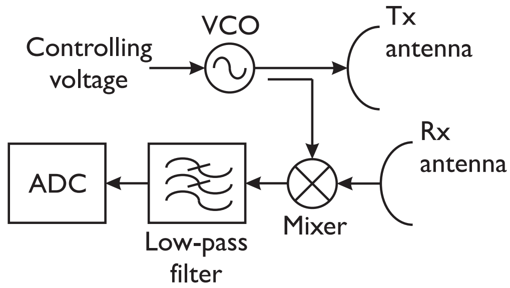

Figure 2. High-level schematic for a biomedical FMCW radar system (Tx: transmission, Rx: reception, VCO: voltage-controlled oscillator, ADC: analog-to-digital converter).

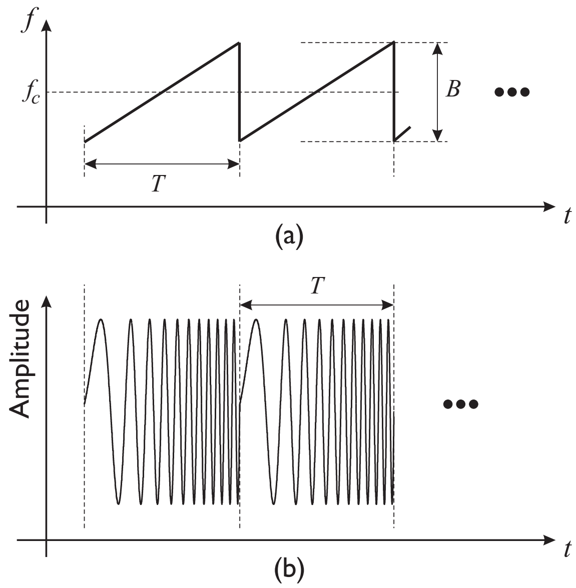

Figure 3. Transmitted waveform for a biomedical FMCW radar. (a) Instantaneous frequency versus time. (b) Amplitude versus time.

The mixing processing in Fig. 2 is referred to as deramping or dechirping [6]. The mixer is not necessarily of quadrature type. Moreover, as previously indicated, the required ADC is a low-end acquisition block with a sampling frequency much lower than the transmitted bandwidth B, as shown below. This opens the possibility to implement FMCW radars at a reduced cost and size.

The complex-valued analytic form of the transmitted signal $s_{Tx}^{B}(t)$ in one period T, where the super-index B refers to this FMCW mode operation, can be written as

$$s_{Tx}^{B}(t) = \exp\left(j\left(2\pi f_c t + \pi\gamma t^2\right)\right) \tag{5}$$

where f_c is the center frequency, γ is the chirp rate—i.e., $\gamma = B/T$, the slope of the linear trend in Fig. 3(a)—, and t is the fast time defined in the interval $[-T/2, T/2]$. A unity amplitude has been again considered.

Assume that the deramping-based biomedical FMCW radar illuminates a moving point-scatterer target whose range is given by $R(\tau)$, where τ is the slow time. After the low-pass filtering in Fig. 2, the baseband beat signal $s_b^B(t)$ for the illuminated point scatterer has the following expression in the interval T

$$s_b^B(t) = s_{Tx}^B(t) \cdot \left(s_{Rx}^B(t)\right)^* \\ = \sigma \exp\left(j\left(\frac{4\pi\gamma R(\tau)}{c}t + \frac{4\pi f_c}{c}R(\tau)\right)\right). \tag{6}$$

The application of a fast Fourier transform (FFT) to the acquired beat signal in the period T permits to obtain its associated range profile. The explanation for this is found in (6) that shows that the frequency of the beat signal is $f_b = 2\gamma R(\tau)/c$, which is proportional to the absolute range of the target $R(\tau)$. In addition, note that the maximum frequency of the beat signal is $f_{b,\max} = 2\gamma R_{\max}/c$, where $R_{\max}$ is the maximum range from which echoes are expected to come. This baseband bandwidth is much lower than the instantaneous bandwidth B, which leads to the very desired simplification of the acquisition ADC without compromising the range resolution of the radar $\Delta_R = c/(2B)$.

Note that the slow-time phase history $\phi(\tau)$ of the second summand in (6) is related to the range history of the biomedical signal, similarly to the case of the Doppler radar. If the coherence feature is maintained, the desired range can be extracted after applying the following expression:

$$\hat{R}(\tau) = \frac{c}{4\pi f_0}\phi(\tau) \tag{7}$$

which is very analogous to (4). In contrast to Doppler radars, the advantage of using a coherent FMCW radar to reconstruct vital signs is that range isolation of the human subject is possible. Other signals in other ranges from other persons or from moving clutter can be thus filtered out.

3 Experimental Results

Fig. 4 shows the photograph of a custom-designed hybrid radar working at C band ($f_0 = 5.8$ GHz) [5]. The micro-controller unit (MCU) selects the Doppler mode as operational function. The architecture for the Doppler radar is a low-IF scheme with the intermediate frequency being 32 Hz. Hence, flicker noise and undesired DC offsets are minimized. The two baseband channels I and Q are sampled by an audio card (i.e., sampling frequency of 44.1 kHz). As radiating subsystems, 2×2 patch antennas are employed for transmission and reception.

The Doppler radar system in Fig. 4 was used to detect the respiration and heartbeat rates of a human subject. The person sat at a distance of about 1.5 m from the radar. He stayed stationary while breathing normally. The respiration rate of the subject was about 13 cycles/min, whereas the

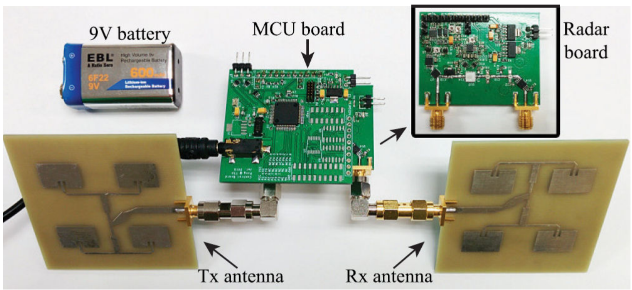

Figure 4. Photograph of a Doppler radar prototype (MCU: micro-controller unit, Tx: transmission, Rx: reception) [5].

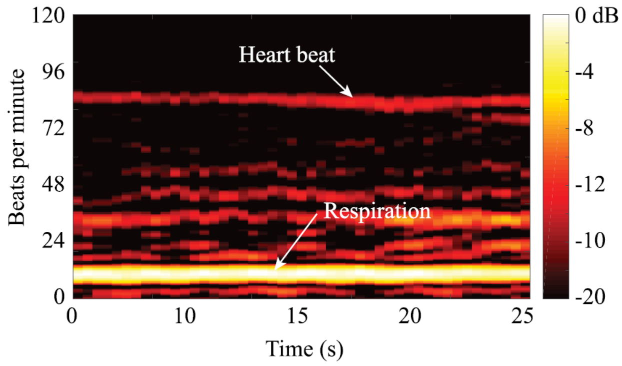

Figure 5. Spectrogram of vital signs extracted by the Doppler radar prototype [5].

heartbeat frequency was about 85 beats/min. Fig. 5 shows the spectrogram calculated for the baseband signal phase. As can be observed, two bright echoes indicate the temporal evolution of the respiration and heartbeat frequencies. The rest of returns in Fig. 5 are secondary lobes and respiration harmonics.

A photograph of a custom-designed coherent deramping-based FMCW radar is provided in Fig. 6 [6]. The center frequency of the ramps is $f_c = 5.8$ GHz. The transmitted bandwidth is $B = 160$ MHz, which leads to a range resolution of $\Delta_R = 0.94$ m. On the other hand, the slow-time sampling period is $T = 2$ ms, which is large enough to adequately sample the slow vital signs. The baseband beat signal is acquired by an audio card and two patch antennas are used for the transmission and reception front ends.

The FMCW radar prototype in Fig. 6 was used to illuminate a stationary human subject breathing normally at a distance of about 1.5 m. The estimated phase-based range is shown in Fig. 7. As observed, the respiration cycles are clearly identifiable. Whereas the FMCW radar is less sensitive and hence the heartbeat signal was not detected, it has range-isolation capabilities coming from the fact that instantaneous bandwidth was transmitted and processed.

4 Conclusions

Non-contact detection and/or monitoring of vital signs has important applications on biomedical and healthcare sce-

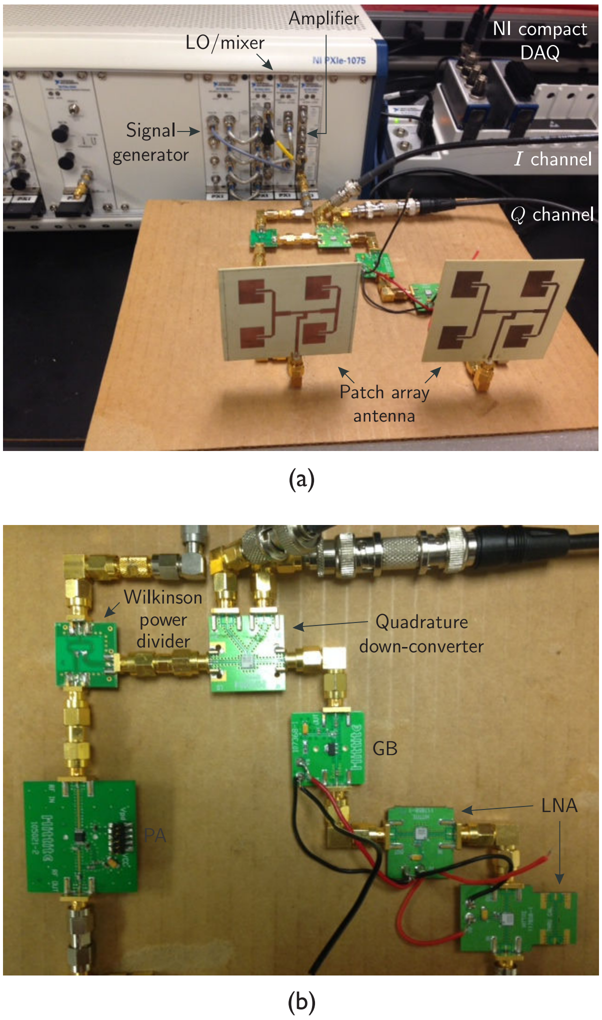

Figure 6. Photograph of an FMCW radar prototype (LNA: low-noise amplifier, DAQ: data acquisition, GB: gain block, NI: National Instruments, LO: local oscillator) [6]. (a) Complete view. (b) Detail.

narios. Traditionally, Doppler radars have been proposed for this task due to their high sensitivity to vibrations. However, these systems have limitations, especially to tolerate moving clutter and to manage several simultaneously-illuminated persons. These drawbacks can be overcome by recently-proposed coherent deramping-based frequency-modulated continuous-wave (FMCW) radars. This article reports the mathematical frameworks of biomedical Doppler and FMCW radar systems, emphasizes their features, and shows some experimental results obtained from custom-designed radar prototypes.

5 Acknowledgements

The work of J.-M. Muñoz-Ferreras and R. Gómez-García was financially supported by the Spanish Ministry of Economy and Competitiveness under Project TEC2017-82398-R. The work of J. Wang, Z. Peng, and C. Li was financially supported by the National Science Foundation under Projects ECCS-1254838 and CNS-1718483.

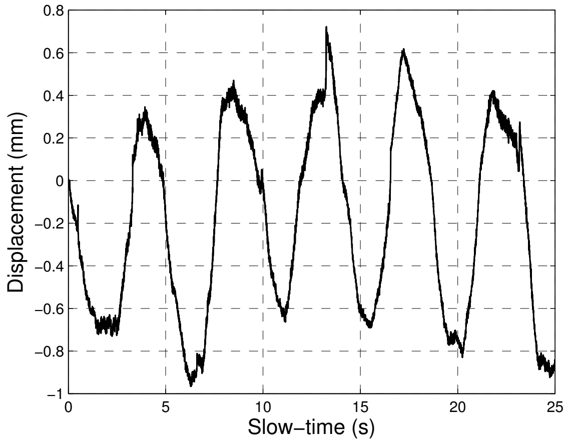

Figure 7. Monitored human respiration pattern obtained by the FMCW radar prototype.

References

[1] C. Li, V. M. Lubecke, O. Boric-Lubecke, and J. Lin, "A review on recent advances in Doppler radar sensors for noncontact healthcare monitoring," *IEEE Trans. Microw. Theory Tech.*, vol. 61, no. 5, pp. 2046–2060, May 2013.

[2] L. Ren, L. Kong, F. Foroughian, H. Wang, P. Theilmann, and A. E. Fathy, "Comparison study of noncontact vital signs detection using a Doppler stepped-frequency continuous-wave radar and camera-based imaging photoplethysmography," *IEEE Trans. Microw. Theory Techn.*, vol. 65, no. 9, pp. 3519–3529, Sep. 2017.

[3] C. Li, Z. Peng, T.-Y. Huang, T. Fan, F.-K. Wang, T.-S. Horng, J.-M. Muñoz-Ferreras, R. Gómez-García, L. Ran, and J. Lin, "A review on recent progress of portable short-range non-contact microwave radar systems," *IEEE Trans. Microw. Theory Techn.*, vol. 65, no. 5, pp. 1692–1706, May 2017.

[4] J. C. Lin, "Noninvasive microwave measurement of respiration," *Proc. IEEE*, vol. 63, no. 10, pp. 1530–1530, Oct. 1975.

[5] Z. Peng, J.-M. Muñoz-Ferreras, Y. Tang, C. Liu, R. Gómez-García, L. Ran, and C. Li, "A portable FMCW-interferometric hybrid radar with programmable low-IF architecture for short-range localization and vital sign tracking," *IEEE Trans. Microw. Theory Techn.*, vol. 65, no. 4, pp. 1334–1344, Apr. 2017.

[6] G. Wang, J.-M. Muñoz-Ferreras, C. Gu, C. Li, and R. Gómez-García, "Application of linear-frequency-modulated continuous-wave (LFMCW) radars for tracking of vital signs," *IEEE Trans. Microw. Theory Techn.*, vol. 62, no. 6, pp. 1387–1399, Jun. 2014.